Chemistry and Physics of Lipids 219 (2019) 50–57

Contents lists available at ScienceDirect

Chemistry and Physics of Lipids

journal homepage: www.elsevier.com/locate/chemphyslip

Detergent-free solubilization of human Kv channels expressed in mammalian cells

M.G. Karlova[a], N. Voskoboynikova[b], G.S. Gluhov[a], D. Abramochkin[a,c], O.A. Malak[d], A. Mulkidzhanyan[b], G. Loussouarn[d], H.-J. Steinhoff[b], K.V. Shaitan[a], O.S. Sokolova[a,*]

[a] Department of Biology, Moscow Lomonosov State University, 119234, Moscow, Russia
[b] Department of Physics, University of Osnabrück, 49069, Osnabrück, Germany
[c] Laboratory of Cardiac Physiology, Institute of Physiology, Komi Science Center, Ural Branch, Russian Academy of Sciences, Syktyvkar, Russia
[d] INSERM, CNRS, l'Institut du Thorax, Université de Nantes, 44007, Nantes, France

ARTICLE INFO

Keywords:
Human Kv channels
hKCNE1-hKCNQ1 complex
SMALP
Electron microscopy
Dynamic light scattering
Affinity purification

ABSTRACT

Styrene-maleic acid (SMA) copolymers are used to extract lipid-encased membrane proteins from lipid bilayers in a detergent-free manner, yielding SMA lipid particles (SMALPs). SMALPs can serve as stable water-soluble nanocontainers for structural and functional studies of membrane proteins. Here, we used SMA copolymers to study full-length pore-forming α-subunits hKCNH5 and hKCNQ1 of human neuronal and cardiac voltage-gated potassium (Kv) channels, as well as the fusion construct comprising of an α-subunit hKCNQ1 and its regulatory transmembrane KCNE1 β-subunit (hKCNE1-hKCNQ1) with added affinity tags, expressed in mammalian COS-1 cells. All these recombinant proteins were shown to be functionally active. Treatment with the SMA copolymer, followed by purification on the affinity column, enabled extraction of all three channels. A DLS experiment demonstrated that negative stain electron microscopy and single particle image analysis revealed a four-fold symmetry within channel-containing SMALPs, which indicates that purified hKCNH5 and hKCNQ1 channels, as well as the hKCNE1-hKCNQ1 fusion construct, retained their structural integrity as tetramers.

1. Introduction

Potassium (K^+) channels control K^+ uptake and efflux in cells (Yellen, 2002; Kuang et al., 2015) and constitute one of the ubiquitous and most diverse classes of membrane proteins (MPs). Voltage-gated K^+ channels (Kv channels), found in all animal cells, compose their largest group and are represented by twelve families (Kv1-Kv12) (Yu et al., 2005). Kv channels are essential for the function of excitable cells (Yellen, 2002), and, thus, for the maintenance of cardiac activity (Wang and MacKinnon, 2017). They are important for the regulation of apoptosis (Pal et al., 2003), cell growth and differentiation (Deutsch and Chen, 1993), and for the release of neurotransmitters (Singer-Lahat et al., 2008) and hormones (MacDonald and Wheeler, 2003). Malfunction of Kv channels leads to severe genetic disorders (Wagner, 2009) and pathological conditions such as neurological disorders (Watanabe et al., 2000) and heart arrhythmias (Tester and Ackerman, 2014). Kv channels are also involved in the pathogenesis of multiple sclerosis (Judge et al., 2006) and in the development of tumors (Camacho, 2006). As far as activators and blockers can modulate the function of Kv channels (Milescu et al., 2013), the latter represent promising drug targets (Thomas et al., 2004; Ikeda et al., 2010). Hence, unraveling the functional mechanism of Kv channels based on their structures is an important task.

Methods of structural biology allow to preform detailed analyses of conformational rearrangements during re-/deactivation of Kv channels using their three-dimensional (3D) structure (Jensen et al., 2012). However, only a few 3D structures of Kv channels are known from X-ray crystallography (Long et al., 2007; Jiang et al., 2003). Recently, single particle electron microscopy (EM) provided high resolution structures of detergent-solubilized ion channels, including the rat Kv10.1 (Eag1) (Whicher and MacKinnon, 2016), the human Kv11.1 (herg) (Wang and MacKinnon, 2017), and the mouse TRPC4 (Duan et al., 2018) channels. Detergents, however, can negatively affect protein stability and activity leading to conformational modifications or even inactivation of MPs (De Zorzi et al., 2016).

A recently developed membrane mimetic system composed of so-called nanodiscs (Bayburt et al., 2002) was successfully applied to structural studies of mammalian ion channels, such as the rat TRPV1 (Gao et al., 2016), the human TRPM4 (Autzen et al., 2018), the mouse endolysosomal TRPML1 (Chen et al., 2017), the Kv1.2–2.1 paddle

* Corresponding author at: 1 Leninskie Gory, bld 12, 119234, Moscow, Russia.
E-mail address: sokolova@mail.bio.msu.ru (O.S. Sokolova).

https://doi.org/10.1016/j.chemphyslip.2019.01.013
Received 31 October 2018; Received in revised form 30 January 2019; Accepted 30 January 2019
Available online 31 January 2019
0009-3084/

chimera channels (Long et al., 2007; Matthies et al., 2018), and the full-length α-subunit of the human Kv7.1 (hKCNQ1) (Shenkarev et al., 2018). Moreover, *in vitro* translation of small viral (Kcv) and bacterial (KcsA and Fluc-Ec2) channels into nanodiscs, followed by their direct reconstitution from these nanoparticles into standard bilayers, was suggested as a valuable tool for functional studies (Winterstein et al., 2018). Detergents are not required in a novel alternative approach, which utilizes amphipathic styrene-maleic acid (SMA) copolymers to solubilize integral MPs by direct extraction from natural membranes or artificial bilayers with given lipid composition (reviewed, e.g., in (Dorr et al., 2016; Lee et al., 2016a, b)). SMA copolymers are non-selective in regard to the lipid type (Arenas et al., 2016; Dominguez Pardo et al., 2017). Soluble SMA lipoprotein particles (SMALPs) consist of a lipid/protein core surrounded by a stabilizing SMA copolymer belt with diameters of about 10 nm (Lee et al., 2016a, 2016b). SMA copolymers were shown to extract both the α-helical bundle (Knowles et al., 2009; Orwick-Rydmark et al., 2012) and β-barrel proteins (Knowles et al., 2009), which maintain protein integrity and activity. Moreover, SMA copolymers can solubilize entire membrane protein complexes (Long et al., 2013; Swainsbury et al., 2014; Dorr et al., 2014; Bell et al., 2015; Voskoboynikova et al., 2017). The small size and single-particle character of SMALPs simplified their structural studies using EM techniques (Postis et al., 2015; Parmar et al., 2018).

In this study, we report the first application of the detergent-free SMA copolymer-based approach to isolate the pore-forming α-subunits hKCNH5 and hKCNQ1 of human Kv channels from mammalian cells. Most mammalian ion channels contain not only the pore-forming subunits, but also the regulatory ones. Therefore, preparations for structural studies that contain both types of subunits are highly desirable. In this work, we further isolated the fusion construct of the hKCNQ1 α-subunit and its auxiliary regulatory KCNE1 β-subunit through direct solubilization of COS-1 cells by SMA, and, subsequently, analyzed three types of the resulting SMALPs by EM.

2. Methods

2.1. Plasmid construction

pIRES2-EGFP/hKCNQ1-1D4. The sequence of the human potassium channel α-subunit hKCNQ1 was amplified from the pCI/KCNQ1 plasmid by PCR. The forward primer was CGCAAATGGGCGGTAGGC GTG. The C-terminal Rho1D4-tag was introduced to the sequence using the reverse primer AATGGATCCTCATGCCGGAGCTACTTGTGAAGTTT CGGTGGACCCCTCATCGG. The PCR mix contained 1M betaine (Sigma-Aldrich) to overcome the excess of GC-pairs in the matrix. The PCR product was ligated into the pIRES2-EGFP vector between EcoRI and BamHI sites.

pcDNA6-V5-HisA/hKCNE1-hKCNQ1. The sequence of the fusion construct containing human KCNE1 subunit fused directly to the N-terminus of the hKCNQ1 subunit was cloned from the pcDNA3.1(-)/hKCNE1-hKCNQ1 plasmid (Wang et al., 1998) with the forward primer CGCAAATGGGCGGTAGGCGTG and the reverse primer CATCT ATTCGAAGGACCCCTCATCGGG. The PCR product was ligated into the pcDNA6/V5-His (A) vector (Invitrogen) between NheI and BstBI restriction sites, in frame with the V5 epitope tag and a 6-histidine Ni-binding tag.

The pMT3-hKCNH5-1D4 vector was a gift from Dr. D. Wray from Leeds University, UK.

2.2. Cell cultures and protein expression

The COS-1 and CHO cell lines were maintained in Dulbecco's modified Eagle's medium (PanEco, Russia), supplemented with 10% of fetal bovine serum (HyClone, USA). COS-7 cells (American Type Culture Collection) were cultured in Dulbecco's modified Eagle's medium (Invitrogen), supplemented with 10% fetal calf serum (Eurobio) and antibiotics (100 IU/ml penicillin and 100 μg/ml streptomycin; Gibco). All cell lines were cultured at 5% CO_2 and 37 °C in a humidified incubator.

Cells were transiently transfected with plasmids pIRES2-EGFP/hKCNQ1-1D4, pcDNA6-V5-HisA/hKCNE1-hKCNQ1 and pMT3-hKCNH5 using the Metafectene PRO (Biontex, Germany) for purification purposes and the Fugene 6 Transfection Reagent (Promega) for the electrophysiological experiments. Cells were split 24 h before transfection. Plasmid DNA was mixed 1:2 with Metafectene PRO or 1:3 with Fugene 6, and added to the cell monolayer grown up to 80% confluency. 48 h after the transfection, cells were subjected to electrophysiological experiments or harvested for further protein purification.

For protein purification, cells were washed twice with a cold PBS supplemented with protease inhibitor cocktail (1 tablet per 50 ml) (Roche, Switzerland), harvested using a cell scraper, frozen in liquid nitrogen and kept at −80 °C until use. Protein expression was assessed with 10% SDS-PAGE and immunoblotting using mouse monoclonal antibody against Rho-1D4 tag, rabbit polyclonal antobody against hKCNQ1 protein and rabbit polyclonal antobody against hKCNE1 protein as primary antibodies (all from Abcam, UK). The secondary antibodies were anti-rabbit (H + L) HRP-conjugated, anti-mouse (H + L) HRP-conjugated and anti-mouse (H + L) AP-conjugated (all from BioRad, USA). Registration of the chemiluminescent or colorimetric signal was performed on the ChemiDoc XRS + imager using ImageLab software (BioRad).

2.3. Single-cell electrophysiology

In transfected mammalian cells, currents were recorded using the whole-cell configuration of the patch-clamp technique. The COS-7 cells were continuously superfused with a HEPES-buffered Tyrode solution containing (in mM): NaCl 145, KCl 4, $MgCl_2$ 1, $CaCl_2$ 1, HEPES 5, glucose 5, pH adjusted to 7.4 with NaOH. The CHO cells were superfused with an external saline solution containing (in mM): NaCl 150, KCl 5.4, $CaCl_2$ 1.8, $MgCl_2$ 1.2, glucose 10, HEPES 10, with pH adjusted to 7.4. Currents were recorded at room temperature (24 ± 1 °C) The cells were visually controlled using Nikon Ti-S inverted luminescent microscope (Tokyo, Japan).

The hKCNE1-hKCNQ1 current density was measured with patch pipettes (Kimble Chase; tip resistance: 1.8 to 2.5 MΩ) filled with an intracellular medium containing (in mM): 100 KCl, 45 K gluconate, 1 $MgCl_2$, 5 EGTA, 10 HEPES, pH adjusted to 7.2 with KOH. All products were purchased from Sigma. Stimulation and data recording were performed with Axon pClamp 10 through an A/D converter (Digidata 1440 A), using an Axopatch 200B amplifier (all Molecular Devices). The current density was measured using depolarizations from a holding potential of −80 mV to various potentials from −60 mV to +80 mV for 4 s and repolarization to −40 mV for 1.2 s where the tail current was measured (increment: 20 mV, stimulation frequency: 0.125 Hz). The Boltzmann fit of the non-normalized activation curves was used to estimate the full-activated hKCNE1-hKCNQ1 current density for each cell.

To measure hKCNQ1 current density, the patch pipettes of 1.5–2.5 MΩ resistance were pulled from borosilicate glass (Sutter Instrument, Novato, CA, USA) and filled with K^+-based electrode solution containing (in mM): 140 KCl, 1 $MgCl_2$, 5 EGTA, 4 MgATP, 0.3 Na_2GTP and 10 HEPES with pH adjusted to 7.2 with KOH. Series resistance and capacitances of pipette and cell were routinely compensated. Current amplitudes were normalized to the capacitive cell size (pA/pF). The potassium current was elicited by a double-pulse protocol from the holding potential of −40 mV by 2 s depolarizing pulses from -20 mV to +80 mV in 20 mV steps followed by 3 s repolarization to −40 mV.

2.4. SMA solution preparation

The styrene maleic acid (SMA) copolymer with a styrene-to-maleic

acid molar ratio of 3:1 (MW 9500 Da, supplied as an aqueous sodium salt solution SMA 3000 HNa) was kindly provided as a gift by Cray Valley (Exton; PA; USA). The 5% (w/v) solution of SMA, which was extensively dialyzed against 10 mM Tris-HCl, 150 mM NaCl, pH 8, was used for the preparation of the SMALPs.

2.5. Preparation of protein-containing SMALPs

COS-1 cells expressing ion channel proteins were resuspended in the buffer A (10 mM Tris-HCl, 150 mM NaCl, 2 mM DTT, 1 mM EDTA, protease inhibitor cocktail, pH 8) in the presence of a 2.5% (w/v) SMA copolymer, incubated for 30 min at 4 °C with shaking, sonicated with an ultrasonic sonicator (Branson Ultrasonic Corporation, USA) for 15 s on ice and incubated for an additional 30 min at 4 °C. Suspensions were centrifuged for 15 min at 200,000 *g*. The pellet and supernatant were analysed by SDS-PAGE and immunoblotting. Supernatants were subsequently purified on affinity resin.

2.6. Detergent solubilization of ion channels

The transfected COS-1 cells were resuspended in the buffer A containing 2.5% of the CHAPS detergent and incubated for 1 h at 4 °C with gentle shaking. Unbroken cell nuclei were pelleted using centrifugation for 5 min at 1500 *g*, at 4 °C. The supernatant was centrifuged for 15 min at 200,000 *g*.

2.7. Affinity chromatography

SMA-solubilized hKCNQ1 and hKCNH5 solutions were added to the NHS-activated sepharose, (GE Healthcare, UK) conjugated with monoclonal anti Rho-1D4 antibody, pre-equilibrated with buffer A, and incubated for 2 h at 4 °C with gentle mixing. The suspension was centrifuged at 3000 *g* for 3 min at 4 °C and the supernatant (column flow through) was discarded. The resin was washed with 30 column volumes of buffer B (Buffer A, containing 330 mM NaCl, pH 8). The protein was eluted with the same buffer, supplemented with 0.2 mg/ml Rho1D4 peptide (Almabion, Russia).

The SMA-solubilized hKCNE1-hKCNQ1 solution was added to the anti V5-tag pAb agarose (MBL, Japan), pre-equilibrated with buffer A. The suspension was then incubated for 2 h at 4 °C with gentle mixing. The resin was pelleted with brief centrifugation, and then washed with 30 column volumes of buffer B and an additional 5 column volumes of PBS. The protein was eluted with 2 mg/ml V5 peptide in PBS (MBL, Japan), supplemented with an additional 150 mM NaCl, 40 mM KCl, 2 mM DTT, 1 mM EDTA protease inhibitor cocktail.

Elution fractions were immediately applied to the glow-discharged EM grids and stained with a 1% uranyl acetate solution. Simultaneously, they were analysed by SDS-PAGE and immunoblotting with anti-1D4 and anti-hKCNQ1 antibodies. The effectiveness of solubilization was estimated using ImageLab software (BioRad, USA).

2.8. Transmission electron microscopy

Copper grids (300 mesh formvar/carbon-coated) (Ted Pella, USA) were hydrophilized by glow discharge (−20 mA, 45 s) with Emitech K100X (Quorum Technologies, UK). A fresh protein sample (3 µl) was placed onto the grid and incubated at RT for 30 s. The excess of the sample was removed with filter paper. Grids were then stained twice with a 1% aqueous uranyl acetate solution for 30 s at RT and air-dried.

Micrographs were acquired using an analytical transmission electron microscope Jem-2100 (Jeol, Japan) equipped with a 2 K x 2 K CCD camera Ultrascan 1000XP (Gatan, USA). The microscope was operated at 200 kV in a low dose mode, with a magnification of x40000 and a defocus of 0.5–1.9 µm.

2.9. Image processing

To obtain the 2D projections of purified ion channels on carbon film, 11,240 particles of hKCNH5, 30,000 particles of hKCNQ1 and 16,531 particles of hKCNE1-hKCNQ1 were selected from the corresponded EM images using Boxer and windowed into 100 × 100 pixel images. These images were merged into stacks, filtered, normalized to a standard deviation of 1, and subjected to the Multivariate statistical analysis (MSA) in IMAGIC5 (van Heel et al., 1996). Final 2D classification was accomplished in RELION2.0.5 (Scheres et al., 2005).

2.10. Dynamic light scattering

Dynamic light scattering experiments were performed on a Brookhaven 90 Plus instrument (Brookhaven Instruments Company, USA), in a thermostated cell at 20 °C. The buffer solution was filtered through 0.22 µm membrane filters. The scattered light was recorded at an angle of θ = 90°, the accumulation time of the signal was 1 min. The measurements were repeated 3–5 times and averaged. The mathematical processing of the experimentally recorded autocorrelation functions of the scattered light was carried out using a package of programs provided by the manufacturer.

3. Results

3.1. The full-length human ion channels, expressed in mammalian cells, are functional

We used transient expression in mammalian cells to express the full-length α-subunits of human ion channels hKCNH5 and hKCNQ1, and the fusion protein of hKCNE1 and hKCNQ1 subunits (Fig. 1). The α-subunit hKCNH5 had the 1D4 affinity tag, which resembles the C-terminal 12 amino acids from rhodopsin (Oprian et al., 1987) for affinity purification purposes, as described in (Sokolova et al., 2012). The α-subunit hKCNQ1 was also fused to the 1D4 tag at the C-terminus. To purify the fusion protein hKCNE1-hKCNQ1, we modified it by adding a V5 (GKPIPNPLLGLDST) affinity tag and a 6xHis tag to the hKCNQ1 subunit's C-terminus.

Electrophysiological experiments on single cells, expressing the hKCNQ1 constructs, confirm that the addition of an 1D4 affinity tag does not disturb the channel functioning (Fig. 2A, B). In order to check whether the tags alter the fused channel activity and biophysical properties, we performed electrophysiological experiments on single cells, expressing the hKCNE1-hKCNQ1 fusion. The obtained current was typical of the hKCNE1-hKCNQ1 channel lacking a tag (Fig. 2C). The averaged current density measured at −40 mV, after full activation of the channel, amounted to 61.9 ± 14.0 pA/pF (n = 8). Considering the slight difference in the quantity of transfected plasmids, it was similar to current densities obtained with untagged hKCNE1-hKCNQ1 (Es-Salah-Lamoureux et al., 2016), amounting to 42.2 ± 13.1 pA/pF (n = 15). Analyzing the channel activation also displayed similar voltage dependences of the two constructs: the half-activation potential of the tagged hKCNE1-hKCNQ1 amounted to 24.7 ± 1.5 mV (n = 8) vs.

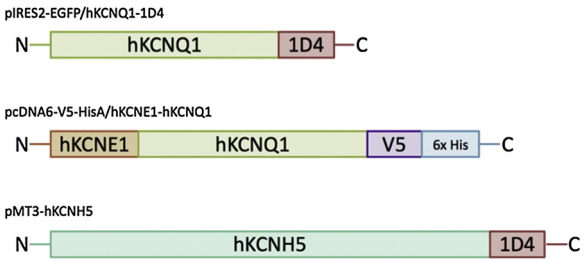

Fig. 1. Schematic representation of the channel expression constructs used in this study.

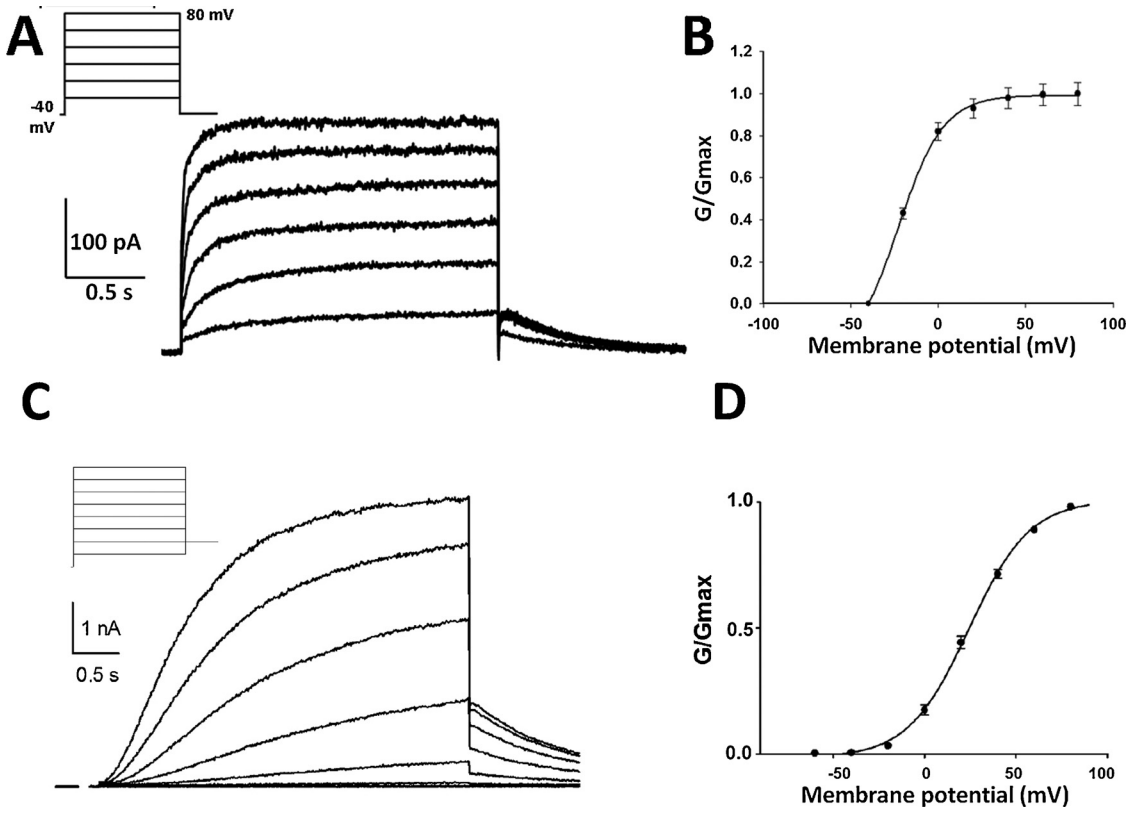

Fig. 2. Expression of functional human ion channels in mammalian cells. (A) Representative superimposed recordings of a CHO cell transfected with pIRES2-EGFP/hKCNQ1-1D4. (B). Mean activation curves of tagged hKCNQ1 (n = 9). (C) Representative superimposed recordings of a COS-7 cell transfected with pCDNA6-V5-His/A-KCNE1-KCNQ1 and GFP as a reporter. Insert: voltage protocol, as detailed in the methods section. (D) Mean activation curves of tagged hKCNE1-hKCNQ1 (n = 8).

24.6 ± 2.3 mV (n = 12) for the untagged hKCNE1-hKCNQ1 (Fig. 2D). The slope of the activation curve was also similar: 15.6 ± 0.5 mV (n = 8) vs. 13.6 ± 0.7 mV (n = 12).

3.2. The full-length human ion channels can be effectively solubilized using SMA

Whole cell membranes readily dissolved upon incubation with a 2.5% SMA solution for 30 min on ice. The suspension, which contained cell debris and DNA, was clarified after sonication and successive centrifugation. We used western blotting on all stages of the solubilization process to check the protein content in the whole cell membranes, solubilized by 2.5% SMA, compared to the detergent (2.5% CHAPS). Immunoblots showed the presence of protein of interest in both the supernatant and the pellet, yet the supernatant solubilization yield achieved with SMA was higher compared to the use of detergent (Table 1).

We then used affinity chromatography on 1D4 or V5 affinity resins to purify human ion channels. The presence of protein of interest in the elution fraction was established by western blot (Figs. 3A and 4 A, B) and electron microscopy (Figs. 3B, 4 C, D). The purified protein was further analyzed by dynamic light scattering (DLS) to assess the average size of assembled protein-containing SMALPs (Fig. 3C). The intensity-weighted particle diameter was estimated to be in the 15-nm range:

Table 1
Solubilization yields of Kv channel proteins, using SMA and detergents.

	Solubilization, %	
Protein	SMA copolymer	CHAPS
KCNQ1	80	40
KCNE1-KCNQ1	15	10

consistent with the average size of the ion channel (15 nm is the diameter of the cytoplasmic part of the EAG-1 channel, while the membrane-embedded part is about 10 nm (Whicher and MacKinnon, 2016)) and previously reported data on SMA-solubilized membranes (Dorr et al., 2016; Knowles et al., 2009; Orwick-Rydmark et al., 2012; Bagrov et al., 2016). The DLS data, thereby, indicate the monodisperse character of the SMALP preparations.

The amount of purified proteins was sufficient for their analyses by negative stain EM. Yet, for high-resolution cryo-EM, much higher concentrations of protein are necessary, so we concentrated one of our samples (hKCNE1-hKCNQ1) on Microcon concentrators (cut-off 30 kDa). It should be noted that the detergent-solubilized protein tends to aggregate under the same conditions (data not shown). For hKCNE1-hKCNQ1, we concentrated 500 µl of combined elution fractions to the final volume of 15 µl. Importantly, the concentrated protein preparation was still monodispersed, according to our EM data.

3.3. Negative stain electron microscopy revealed tetrameric channel particles

Affinity purified ion channels solubilized in SMALPs were studied using a JEOL 2100 microscope at low-dose conditions. 197 images for hKCNQ1, 106 images for hKCNE1-hKCNQ1 and 95 images for hKCNH5 were collected; each field of view contained a large number of particles, 12–15 nm in the diameter, depending on the channel studied (Figs. 3B, 4 C, D). About 37,000 single particles from three data sets were collected semi-automatically using EMAN Boxer; contrast transfer function correction was carried out in EMAN2.1 (Ludtke et al., 1999) and the particle sets were then subjected to reference-free classification in RELION2.0.5 (Scheres et al., 2005). 9354 single particles were used for the final 2D classification of hKCNQ1, 16,531 particles were used for the 2D classification of hKCNE1-hKCNQ1 and 11,240 particles were used

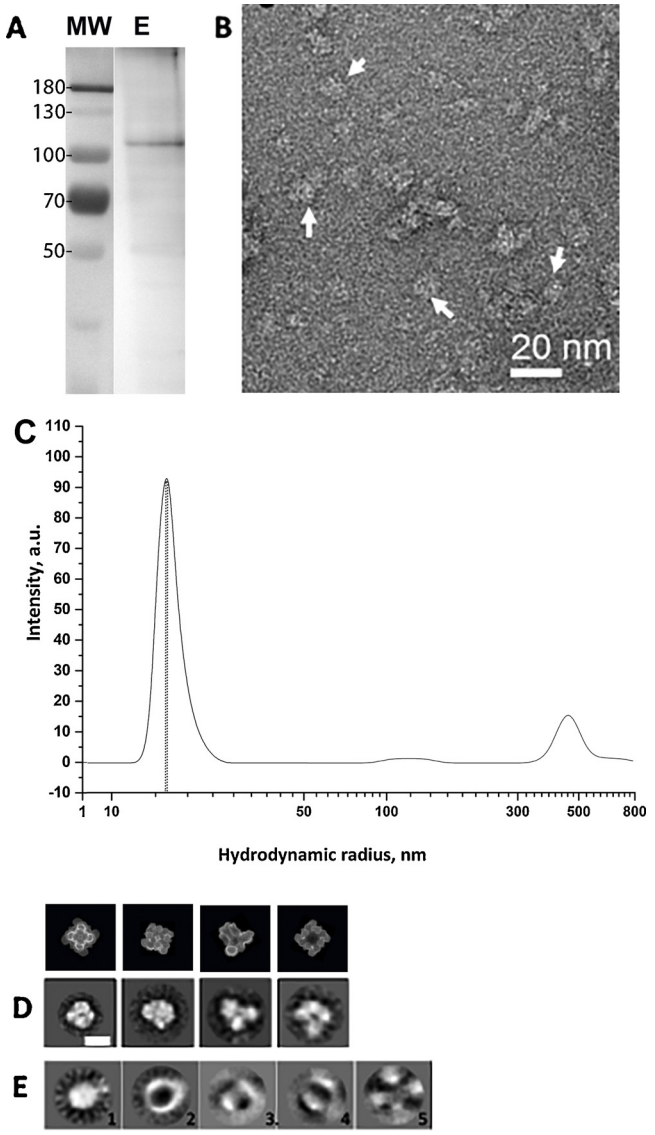

Fig. 3. The solubilization and purification of human ion channel (hKCNH5) by SMA copolymer.

(A) Western blot of elution fraction containing hKCNH5; mouse monoclonal antibody directed against 1D4 tag was used as a primary antibody: MW-protein ladder; E – elution with 1D4 peptide. (B) EM image of the elution fraction, stained with 1% UA. White arrows indicate hKCNH5 particles. Bar size – 20 nm. (C) DLS curve of elution fraction of the hKCNH5 channel. (D) Representative class-averages of hKCNH5. Bar size – 10 nm. Above each 2D average, the corresponded 2D projection of the *Rattus norvegicus* EAG-1 channel structure (EMD-8215) is placed for comparison. (E) Eigenimages generated upon classification of hKCNH5. Images reflect variations in densities of particles related to the different symmetry. Eigenimage #5 demonstrates the presence of four-fold symmetry.

for the 2D classification of hKCNH5. The aligned images were subjected to MSA, where each image was represented as a point in a multi-dimensional space. MSA determines the new coordinate system where each aligned image can be expressed as a linear combination of independent eigenimages. Eigenimages reflect variations in particle densities, in relation to different symmetry. Thus, we could conclude that the projections of the studied channels purified using SMA possess the four-fold symmetry (Fig. 3E, eigenimage #5, Fig. 4G, eigenimage #3, Fig. 4H, eigenimage #2), confirming that they are present in SMALPs as tetramers. The resulting classes displayed projection structures of about 12–15 nm in diameter, depending on the channel (Figs. 3D, 4 E, F). The orientation of the particles on the grid was random, suggesting that the SMA did not affect the preferred interactions of the purified protein with the carbon film, which occurs, e.g., with detergent-solubilized *Shaker* channels (Sokolova et al., 2001).

4. Discussion

Recently, the use of polymer nanodiscs for protein purification became a hot topic. So far, the characterizations in SMALPs were reported for small membrane proteins, including bacterial KcsA (Dorr et al., 2014), ARC-B transporter (Postis et al., 2015) and the human KCNE1 transmembrane subunit (Sahu et al., 2013), expressed in *E. coli*. Information on the use of SMALPs for purification of large eukaryotic channels is limited to the human GPCR (Jamshad et al., 2015) and eukaryotic ABC transporters (Gulati et al., 2014), purified from isolated membrane fractions. Here, we report, for the first time, the application of SMALPs to the solubilization of full-length human Kv channels: pore-forming α-subunits hKCNQ1 and hKCNH5, as well as the complex of the α-subunit hKCNQ1 with its auxiliary subunit hKCNE1. All channels were purified from the COS-1 cell membrane using whole-cell solubilization. The importance of the studied channels is justified by the fact that hKCNQ1 belongs to cardiac voltage-dependent potassium channels, while hKCNH5 is found in the central nervous system (Bauer and Schwarz, 2018).

The structures of homologous channels, Kv7.1 from *Xenopus laevis* (Sun and MacKinnon, 2017) and human Kv10.1 (Eag1) (Whicher and MacKinnon, 2016), were studied using cryo-EM. The flexible parts of both channels bearing Cys residues, including flexible domains and loops, were truncated to prevent aggregation (Sun and MacKinnon, 2017; Whicher and MacKinnon, 2016). Some cytoplasmic regions of the Kv7.1 channel were removed and the final construct contained amino acids from position 67 to 610 (Sun and MacKinnon, 2017). Similarly, 114 amino acid residues at the C-terminus of the Kv10.1 channel were removed (positions 773–886) (Whicher and MacKinnon, 2016). As a result, the truncated channels had slightly altered activation potentials. For correct functioning of the Kv7 channels, phosphatidylinositol 4,5-bisphosphate (PIP_2) is necessary (Loussouarn et al., 2003; Zaydman et al., 2013). However, due to the use of detergent solubilization, followed by chromatography purification, lipids were substituted by detergent and the Kv7.1 channel structure was solved in the absence of PIP_2 in the so-called 'uncoupled' state, with depolarized voltage sensor and a closed pore (Sun and MacKinnon, 2017).

Our first goal here was to express and purify those full-length human channels keeping intact their large cytoplasmic domains and natural lipid environment. We used SMA copolymer for the solubilization of whole mammalian cells to eliminate the use of detergents and to allow one-step affinity purification. This approach allows preserving natural lipids from the mammalian cell membrane in SMALPs, which is especially important when isolating the KCNQ1 channel. Therefore, the presence of PIP_2 lipids in channel-containing SMALPs could likely facilitate the obtaining of the Kv7.1 channel structure with a pore in an opened state.

To our knowledge, some MPs are difficult to solubilize from native sources, which may be due to e.g., a low lipid/protein ratio (Dorr et al., 2016; Routledge et al., 2016). Therefore, usually, during the purification process, it is important to keep the detergent concentration relatively high, because its drop below the critical micelle concentration (CMC) may affect dispersity (Sokolova, 2004) or the correct conformation of the purified channels (Lee et al., 2005). We used transient transfection of the COS-1 cells to overexpress the Kv channels and compared the effectiveness of their solubilization by SMA and detergent (Table 1). We demonstrated that the SMA copolymer was more efficient at solubilization of the human KCNQ1 channels than CHAPS. Detergents have been used before in many structural studies (for review see for example De Zorzi et al., 2016); high-quality preparations for EM could be obtained by using the appropriate detergents and baculovirus

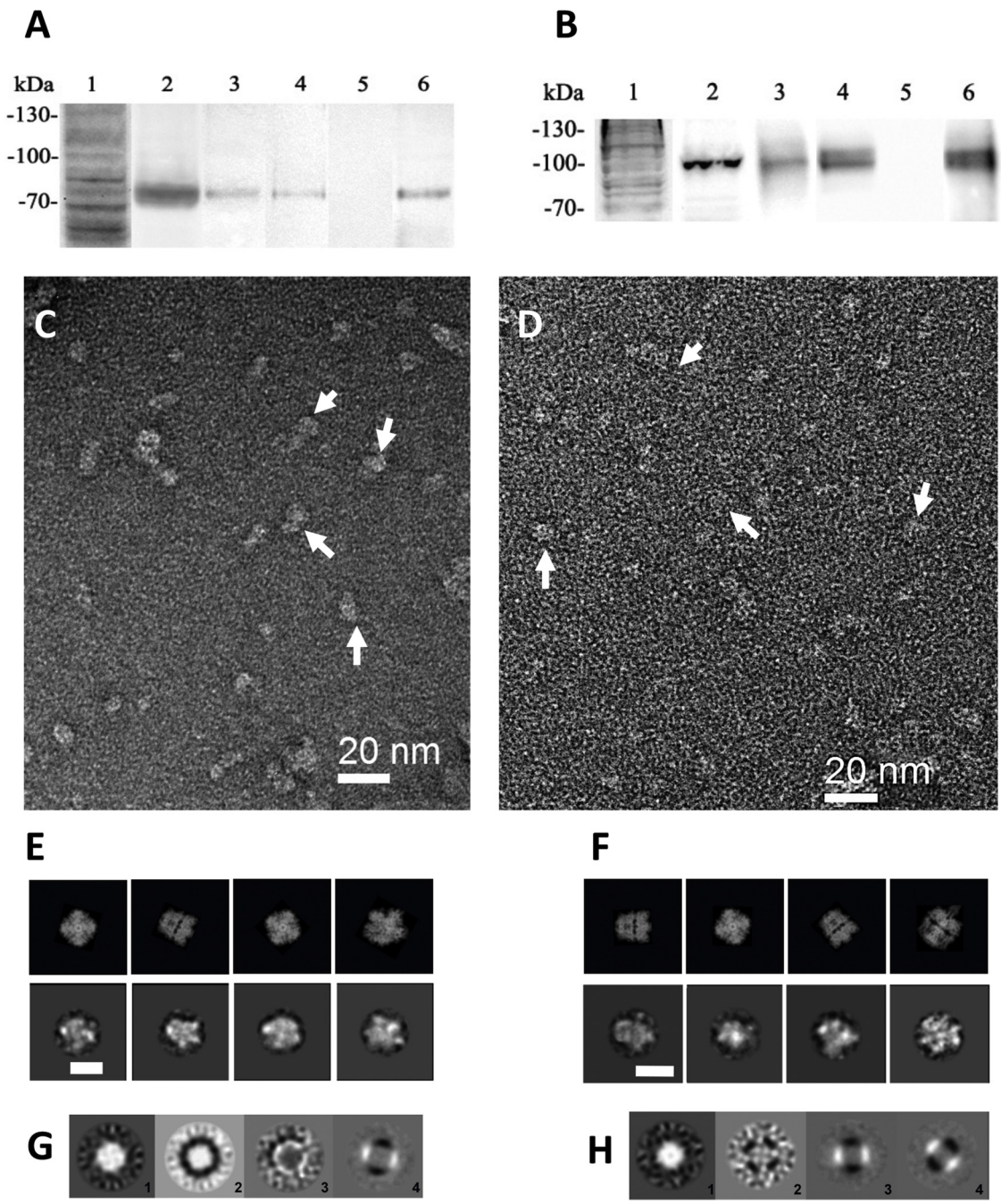

Fig. 4. The solubilization and purification of hKCNQ1 and hKCNE1-hKCNQ1 by SMA copolymer. (A) hKCNQ1 protein expression, solubilization with SMA and purification on anti-1D4 affinity resin. Line 1 - SDS-PAGE of KCNQ1 protein expression in COS-1 cells, coomassie staining; line 2–6 - western blots, immunodetection with anti-1D4 Ab. 2 - COS-1 cells extract; 3 - solubilization with 2.5% of SMA copolymer - supernatant; 4 - pellet; 5 - anti 1D4 column wash; 6 - elution fraction. (B) hKCNE1-hKCNQ1 fusion expression, solubilization with SMA copolymer and purification on the anti-V5 affinity resin. Line 1 - SDS-PAGE of hKCNE1-hKCNQ1 protein expression in COS-1 cells, coomassie staining; line 2–6 - western blots, immunodetection with anti KCNQ1 Ab. 2 - COS-1 cells extract; 3 - solubilization with 2.5% of SMA copolymer - supernatant; 4 - pellet; 5 - anti V5 column wash; 6 - elution fraction. EM images of (C) purified hKCNQ1 and (D) hKCNE1-hKCNQ1, both stained with 1% UA. Arrows indicate channel particles. Bar size – 20 nm; Representative 2D class-averages of (E) hKCNQ1 and (F) hKCNE1-hKCNQ1. Above each 2D average, the corresponded projection of the available *Xenopus laevis* KCNQ1 channel structure (EMD-8712) is placed for comparison. Bar size – 10 nm. Eigenimages, obtained after MSA of (G) hKCNQ1 particles and (H) hKCNE1-hKCNQ1 particles.

expression system (Guo and MacKinnon, 2017). Yet, for channels expressed in mammalian cells, the solubilization in detergent often yielded rather low concentrations. The advantage of using SMALP is that the solubilized membrane proteins can be easily concentrated on Microcon concentrators without aggregation.

Our second goal was to develop a procedure for expression and purification of the complex of the α-subunit hKCNQ1 with its auxiliary subunit hKCNE1 for further cryo-EM experiments. To avoid the structural variability, due to various stoichiometry from one particle to another that may further interfere with image processing, we used the fusion construct, which includes both α- and ß-subunits with the stoichiometry of subunits 4:4 (Choveau et al., 2011; Wang et al., 1998). Single-cell electrophysiological experiments confirmed that this construct was fully active (Fig. 2C). We were able to isolate the complex from mammalian COS-1 cells using SMALPs and to examine its 2D structure. Multivariate statistical analysis on the aligned channel

particles produced eigenimages (Fig. 4H), suggesting either two- or four-fold symmetry, in agreement with current and previous (Shenkarev et al., 2018) data for the α-subunit. Hence, incorporation into SMALPs did not affect the conformation of the purified fusion channel. Moreover, in concordance with earlier reports (Routledge et al., 2016), we found that the SMA-solubilized hKCNE1-hKCNQ1 construct was more stable, less prone to aggregation and easier to concentrate than detergent-solubilized proteins.

In summary, using SMA copolymers, we tested a method of detergent-free solubilization of human ion channels, particularly, the cardiac and neuronal potassium voltage-dependent channels. SMALPs appear to develop into a convenient platform for studying the structure of human ion channels and their complexes (which are hard to crystallize) using not only cryo-EM, but also NMR methods, as well as other structural methods that require using the single particle mode (including XFEL). The study of the structural and functional properties of voltage-dependent potassium channels would help to clarify the mechanisms that cause malfunction of these channels in case of point mutations. Understanding these mechanisms, in its turn, would pave the way to methods of targeted correction of channel function.

Conflicts of interest

The authors have no conflicts of interest.

Acknowledgements

Authors thank Dr. Irina Panova for her help with DLS experiments, Andrey Moiseenko for his help with obtaining the electron microscopy images, Lisa Trifonova for proofreading the manuscript and Béatrice Le Ray for expert technical assistance. Electron microscopy was performed at the user facilities center 'Electron microscopy in the life sciences' of the Biology Department of Lomonosov Moscow State University.

The purification of hKCNQ1 and hKCNE1-hKCNQ1 by a SMA copolymer and their investigations were financially supported by the Russian Foundation for Basic Research (Project #18-504-12045 to K.V.S.); DLS experiments were supported by the German Research Foundation (DFG) (Project #STE640/15 to H.-J.S.). Experiments on the purification of hKCNH5 ion channel and its EM studies were supported by the Russian Science Foundation young investigators grant (Project #18-74-00087 to G.S.G.). The electrophysiological experiments were funded by the Kolmogorov program of the Partenariat Hubert Curien (35503SC) for G.L. and O.A.M. O.A.M. was laureate of the Line Pomaret-Delalande prize of the Fondation pour la Recherche Médicale (PLP20141031304; FRM). O.A.M. wishes to personally thank Mrs. Line Pomaret for her generous support. O.A.M. was supported by the Fondation Génavie.

References

Arenas, R.C., Klingler, J., Vargas, C., Keller, S., 2016. Influence of lipid bilayer properties on nanodisc formation mediated by styrene/maleic acid copolymers. Nanoscale 8, 15016–15026.

Autzen, H.E., Myasnikov, A.G., Campbell, M.G., Asarnow, D., Julius, D., Cheng, Y., 2018. Structure of the human TRPM4 ion channel in a lipid nanodisc. Science 359, 228–232.

Bagrov, D.V., Voskoboynikova, N., Armeev, G.A., Mosslehy, W., Gluhov, G.S., Ismagulova, T.T., Mulkidjanian, A.Y., Kirpichnikov, M.P., Steinhoff, H.-J., Shaitan, K.V., 2016. Characterization of lipodisc nanoparticles containing sensory rhodopsin ii and its cognate transducer from Natronomonas pharaonis. Biofizika (Biophysics) Moscow 61, 942–949.

Bauer, C.K., Schwarz, J.R., 2018. Ether-a-go-go K(+) channels: effective modulators of neuronal excitability. J. Physiol. 596, 769–783.

Bayburt, T.H., Grinkova, Y.V., Sligar, S.G., 2002. Self-assembly of discoidal phospholipid bilayer nanoparticles with membrane scaffold proteins. Nano Lett. 2, 853–856.

Bell, A.J., Frankel, L.K., Bricker, T.M., 2015. High yield non-detergent isolation of photosystem I-lightharvesting chlorophyll II membranes from spinach thylakoids implications for the organization of the PS I antennae in higher plants. J. Biol. Chem. 290, 18429–18437.

Camacho, J., 2006. Ether a go-go potassium channels and cancer. Cancer Lett. 233, 1–9.

Chen, Q., She, J., Zeng, W., Guo, J., Xu, H., Bai, X.C., Jiang, Y., 2017. Structure of mammalian endolysosomal TRPML1 channel in nanodiscs. Nature 550, 415–418.

Choveau, F.S., Rodriguez, N., Abderemane Ali, F., Labro, A.J., Rose, T., Dahimene, S., Boudin, H., Le Henaff, C., Escande, D., Snyders, D.J., Charpentier, F., Merot, J., Baro, I., Loussouarn, G., 2011. KCNQ1 channels voltage dependence through a voltage-dependent binding of the S4-S5 linker to the pore domain. J. Biol. Chem. 286, 707–716.

De Zorzi, R., Mi, W., Liao, M., Walz, T., 2016. Single-particle electron microscopy in the study of membrane protein structure. Microscopy 65, 81–96.

Deutsch, C., Chen, L.Q., 1993. Heterologous expression of specific K+ channels in T lymphocytes: functional consequences for volume regulation. Proc. Natl. Acad. Sci. U. S. A. 90, 10036–10040.

Dominguez Pardo, Juan J., Dorr, J.M., Iyer, A., Cox, R.C., Scheidelaar, S., Koorengevel, M.C., Subramaniam, V., Killian, J.A., 2017. Solubilization of lipids and lipid phases by the styrene-maleic acid copolymer. Eur. Biophys. J. 46, 91–101.

Dorr, J.M., Koorengevel, M.C., Schafer, M., Prokofyev, A.V., Scheidelaar, S., van der Cruijsen, E.A., Dafforn, T.R., Baldus, M., Killian, J.A., 2014. Detergent-free isolation, characterization, and functional reconstitution of a tetrameric K+ channel: the power of native nanodiscs. Proc. Natl. Acad. Sci. U. S. A. 111, 18607–18612.

Dorr, J.M., Scheidelaar, S., Koorengevel, M.C., Dominguez, J.J., Schafer, M., van Walree, C.A., Killian, J.A., 2016. The styrene-maleic acid copolymer: a versatile tool in membrane research. Eur. Biophys. J. 45, 3–21.

Duan, J., Li, J., Zeng, B., Chen, G.L., Peng, X., Zhang, Y., Wang, J., Clapham, D.E., Li, Z., Zhang, J., 2018. Structure of the mouse TRPC4 ion channel. Nat. Commun. 9, 3102.

Es-Salah-Lamoureux, Z., Jouni, M., Malak, O.A., Belbachir, N., Al Sayed, Z.R., Gandon-Renard, M., Lamirault, G., Gauthier, C., Baró, I., Charpentier, F., Zibara, K., Lemarchand, P., Beaumelle, B., Gaborit, N., Loussouarn, G., 2016. HIV-Tat induces a decrease in IKr and IKsvia reduction in phosphatidylinositol-(4,5)-bisphosphate availability. J. Mol. Cell Cardiol. 99, 1–13.

Gao, Y., Cao, E., Julius, D., Cheng, Y., 2016. TRPV1 structures in nanodiscs reveal mechanisms of ligand and lipid action. Nature 534, 347–351.

Gulati, S., Jamshad, M., Knowles, T.J., Morrison, K.A., Downing, R., Cant, N., Collins, R., Koenderink, J.B., Ford, R.C., Overduin, M., Kerr, I.D., Dafforn, T.R., Rothnie, A.J., 2014. Detergent-free purification of ABC (ATP-binding-cassette) transporters. Biochem. J. 461, 269–278.

Guo, Y.R., MacKinnon, R., 2017. Structure-based membrane dome mechanism for Piezo mechanosensitivity. Elife 6.

Ikeda, M., Tomita, Y., Mouri, A., Koga, M., Okochi, T., Yoshimura, R., Yamanouchi, Y., Kinoshita, Y., Hashimoto, R., Williams, H.J., Takeda, M., Nakamura, J., Nabeshima, T., Owen, M.J., O'Donovan, M.C., Honda, H., Arinami, T., Ozaki, N., Iwata, N., 2010. Identification of novel candidate genes for treatment response to risperidone and susceptibility for schizophrenia: integrated analysis among pharmacogenomics, mouse expression, and genetic case-control association approaches. Biol. Psychiatry 67, 263–269.

Jamshad, M., Charlton, J., Lin, Y.P., Routledge, S.J., Bawa, Z., Knowles, T.J., Overduin, M., Dekker, N., Dafforn, T.R., Bill, R.M., Poyner, D.R., Wheatley, M., 2015. G-protein coupled receptor solubilization and purification for biophysical analysis and functional studies, in the total absence of detergent. Biosci. Rep. 35.

Jensen, M.O., Jogini, V., Borhani, D.W., Leffler, A.E., Dror, R.O., Shaw, D.E., 2012. Mechanism of voltage gating in potassium channels. Science 336, 229–233.

Jiang, Y., Lee, A., Chen, J., Ruta, V., Cadene, M., Chait, B.T., MacKinnon, R., 2003. X-ray structure of a voltage-dependent K+ channel. Nature 423, 33–41.

Judge, S.I.V., Lee, J.M., Bever, C.T., Hoffman, P.M., 2006. Voltage-gated potassium channels in multiple sclerosis: Overview and new implications for treatment of central nervous system inflammation and degeneration. J. Rehabil. Res. Dev. 43, 111–121.

Knowles, T.J., Finka, R., Smith, C., Lin, Y.P., Dafforn, T., Overduin, M., 2009. Membrane proteins solubilized intact in lipid containing nanoparticles bounded by styrene maleic acid copolymer. J. Am. Chem. Soc. 131, 7484–7485.

Kuang, Q., Purhonen, P., Hebert, H., 2015. Structure of potassium channels. Cell. Mol. Life Sci.: CMLS 72, 3677–3693.

Lee, S.Y., Lee, A., Chen, J., MacKinnon, R., 2005. Structure of the KvAP voltage-dependent K+ channel and its dependence on the lipid membrane. Proc. Natl. Acad. Sci. U. S. A. 102, 15441–15446.

Lee, S.C., Knowles, T.J., Postis, V.L.G., Jamshad, M., Parslow, R.A., Lin, Y., Goldman, A., Sridhar, P., Overduin, M., Muench, S.P., Dafforn, T.R., 2016a. A method for detergent-free isolation of membrane proteins in their local lipid environment. Nat. Protoc. 11 (7), 1149–1162.

Lee, S.C., Khalid, S., Pollock, N.L., Knowles, T.J., Edler, K., Rothnie, A.J., Thomas, Owen R.T., Dafforn, T.R., 2016b. Encapsulated membrane proteins: a simplified system for molecular simulation. Biochim. Biophys. Acta 1858, 2549–2557.

Long, S.B., Tao, X., Campbell, E.B., MacKinnon, R., 2007. Atomic structure of a voltage-dependent K+ channel in a lipid membrane-like environment. Nature 450, 376–382.

Long, A.R., O'Brien, C.C., Malhotra, K., Schwall, C.T., Albert, A.D., Watts, A., Alder, N.N., 2013. A detergent-free strategy for the reconstitution of active enzyme complexes from native biological membranes into nanoscale discs. BMC Biotechnol. 13.

Loussouarn, G., Park, K.H., Bellocq, C., Baro, I., Charpentier, F., Escande, D., 2003. Phosphatidylinositol-4,5-bisphosphate, PIP2, controls KCNQ1/KCNE1 voltage-gated potassium channels: a functional homology between voltage-gated and inward rectifier K+ channels. EMBO J. 22, 5412–5421.

Ludtke, S.J., Baldwin, P.R., Chiu, W., 1999. EMAN: semiautomated software for high-resolution single-particle reconstructions. J. Struct. Biol. 128, 82–97.

MacDonald, P.E., Wheeler, M.B., 2003. Voltage-dependent K(+) channels in pancreatic beta cells: role, regulation and potential as therapeutic targets. Diabetologia 46, 1046–1062.

Matthies, D., Bae, C., Toombes, G.E., Fox, T., Bartesaghi, A., Subramaniam, S., Swartz,

K.J., 2018. Single-particle cryo-EM structure of a voltage-activated potassium channel in lipid nanodiscs. eLife 7.
Milescu, M., Lee, H.C., Bae, C.H., Kim, J.I., Swartz, K.J., 2013. Opening the shaker K+ channel with hanatoxin. J. Gen. Physiol. 141, 203–216.
Oprian, D.D., Molday, R.S., Kaufman, R.J., Khorana, H.G., 1987. Expression of a synthetic bovine rhodopsin gene in monkey kidney cells. Proc. Natl. Acad. Sci. U. S. A. 84, 8874–8878.
Orwick-Rydmark, M., Lovett, J.E., Graziadei, A., Lindholm, L., Hicks, M.R., Watts, A., 2012. Detergent-free incorporation of a seven-transmembrane receptor protein into nanosized bilayer Lipodisq particles for functional and biophysical studies. Nano Lett. 12, 4687–4692.
Pal, S., Hartnett, K.A., Nerbonne, J.M., Levitan, E.S., Aizenman, E., 2003. Mediation of neuronal apoptosis by Kv2.1-encoded potassium channels. J. Neurosci. 23, 4798–4802.
Parmar, M., Rawson, S., Scarff, C.A., Goldman, A., Dafforn, T.R., Muench, S.P., Postis, V.L.G., 2018. Using a SMALP platform to determine a sub-nm single particle cryo-EM membrane protein structure. Biochim. Biophys. Acta 1860, 378–383.
Postis, V., Rawson, S., Mitchell, J.K., Lee, S.C., Parslow, R.A., Dafforn, T.R., Baldwin, S.A., Muench, S.P., 2015. The use of SMALPs as a novel membrane protein scaffold for structure study by negative stain electron microscopy. Biochim. Biophys. Acta 1848, 496–501.
Routledge, S.J., Mikaliunaite, L., Patel, A., Clare, M., Cartwright, S.P., Bawa, Z., Wilks, M.D., Low, F., Hardy, D., Rothnie, A.J., Bill, R.M., 2016. The synthesis of recombinant membrane proteins in yeast for structural studies. Methods 95, 26–37.
Sahu, I.D., McCarrick, R.M., Troxel, K.R., Zhang, R.F., Smith, H.J., Dunagan, M.M., Swartz, M.S., Rajan, P.V., Kroncke, B.M., Sanders, C.R., Lorigan, G.A., 2013. DEER EPR measurements for membrane protein structures via bifunctional spin labels and lipodisq nanoparticles. Biochemistry 52, 6627–6632.
Scheres, S.H., Valle, M., Nunez, R., Sorzano, C.O., Marabini, R., Herman, G.T., Carazo, J.M., 2005. Maximum-likelihood multi-reference refinement for electron microscopy images. J. Mol. Biol. 348, 139–149.
Shenkarev, Z.O., Karlova, M.G., Kulbatskii, D.S., Kirpichnikov, M.P., Lyukmanova, E.N., Sokolova, O.S., 2018. Recombinant production, reconstruction in lipid-protein nanodiscs, and electron microscopy of full-length alpha-subunit of human potassium channel Kv7.1. Biochemistry 83, 562–573.
Singer-Lahat, D., Chikvashvili, D., Lotan, I., 2008. Direct interaction of endogenous Kv channels with syntaxin enhances exocytosis by neuroendocrine cells. PLoS One 3, e1381.
Sokolova, O., 2004. Structure of cation channels, revealed by single particle electron microscopy. FEBS Lett. 564, 251–256.
Sokolova, O., Kolmakova-Partensky, L., Grigorieff, N., 2001. Three-dimensional structure of a voltage-gated potassium channel at 2.5 nm resolution. Structure 9, 215–220.
Sokolova, O.S., Shaitan, K.V., Grizel, A.V., Popinako, A.V., Karlova, M.G., Kirpichnikov, M.P., 2012. Three-dimensional structure of human Kv10.2 ion channel studied by single particle electron microscopy and molecular modeling. Bioorg. Khim. 38, 177–184.
Sun, J., MacKinnon, R., 2017. Cryo-EM structure of a KCNQ1/CaM complex reveals insights into congenital long QT syndrome. Cell 169, 1042–1050 e9.
Swainsbury, D.J., Scheidelaar, S., van Grondelle, R., Killian, J.A., Jones, M.R., 2014. Bacterial reaction centers purified with styrene maleic acid copolymer retain native membrane functional properties and display enhanced stability. Angew. Chem. Int. Ed. Engl. 53, 11803–11807.
Tester, D.J., Ackerman, M.J., 2014. Genetics of long QT syndrome. Methodist Debakey Cardiovasc. J. 10, 29–33.
Thomas, D., Wimmer, A.B., Wu, K., Hammerling, B.C., Ficker, E.K., Kuryshev, Y.A., Kiehn, J., Katus, H.A., Schoels, W., Karle, C.A., 2004. Inhibition of human ether-a-go-go-related gene potassium channels by alpha 1-adrenoceptor antagonists prazosin, doxazosin, and terazosin. Naunyn Schmiedebergs Arch. Pharmacol. 369, 462–472.
van Heel, M., Harauz, G., Orlova, E.V., Schmidt, R., Schatz, M., 1996. A new generation of the IMAGIC image processing system. J. Struct. Biol. 116, 17–24.
Voskoboynikova, N., Mosslehy, W., Colbasevici, A., Ismagulova, T.T., Bagrov, D.V., Akovantseva, A.A., Timashev, P.S., Mulkidjanian, A.Y., Bagratashvili, V.N., Shaitan, K.V., Kirpichnikov, M.P., Steinhoff, H.J., 2017. Characterization of an archaeal photoreceptor/transducer complex from *Natronomonas pharaonis* assembled within styrene-maleic acid lipid particles. RSC Adv. 7, 51324–51334.
Wagner, D.T., 2009. Palliative hypofractionated radiotherapy for non-small cell lung cancer (NSCLC) patients previously treated by induction chemotherapy: is it for many, some, all, or none? J. Thorac. Dis. 1, 1–2.
Wang, W., MacKinnon, R., 2017. Cryo-EM Structure of the Open Human Ether-a-go-go-Related K(+) Channel hERG. Cell 169, 422–430 e10.
Wang, W., Xia, J., Kass, R.S., 1998. MinK-KvLQT1 fusion proteins, evidence for multiple stoichiometries of the assembled IsK channel. J. Biol. Chem. 273, 34069–34074.
Watanabe, H., Nagata, E., Kosakai, A., Nakamura, M., Yokoyama, M., Tanaka, K., Sasai, H., 2000. Disruption of the epilepsy KCNQ2 gene results in neural hyperexcitability. J. Neurochem. 75, 28–33.
Whicher, J.R., MacKinnon, R., 2016. Structure of the voltage-gated K(+) channel Eag1 reveals an alternative voltage sensing mechanism. Science 353, 664–669.
Winterstein, L.M., et al., 2018. Reconstitution and functional characterization of ion channels from nanodiscs in lipid bilayers. J. Gen. Physiol. 150, 637–646.
Yellen, G., 2002. The voltage-gated potassium channels and their relatives. Nature 419, 35–42.
Yu, F.H., Yarov-Yarovoy, V., Gutman, G.A., Catterall, W.A., 2005. Overview of molecular relationships in the voltage-gated ion channel superfamily. Pharmacol. Rev. 57, 387–395.
Zaydman, M.A., Silva, J.R., Delaloye, K., Li, Y., Liang, H., Larsson, H.P., Shi, J., Cui, J., 2013. Kv7.1 ion channels require a lipid to couple voltage sensing to pore opening. Proc. Natl. Acad. Sci. U. S. A. 110, 13180–13185.